

POSSIBLE GEOMETRIC PATTERNS IN $0.1c$ SCALE STRUCTURE

R. BRENT TULLY

Institute for Astronomy, University of Hawaii, 2680 Woodlawn Drive, Honolulu, HI 96822,¹ and Istituto di Radioastronomia/
 Consiglio Nazionale delle Ricerche, via Irnerio 46, 40126 Bologna, Italy

ROBERTO SCARAMELLA

Osservatorio Astronomico di Roma, 00040 Monteporzio Catone, Italy

GIAMPAOLO VETTOLANI

Istituto di Radioastronomia/Consiglio Nazionale delle Ricerche, via Irnerio 46, 40126 Bologna, Italy

AND

GIOVANNI ZAMORANI

Osservatorio Astronomico, via Zamboni 33, 40126 Bologna, Italy;¹ and Istituto di Radioastronomia/Consiglio Nazionale delle Ricerche,
 via Irnerio 46, 40126 Bologna, Italy

Received 1991 July 23; accepted 1991 September 27

ABSTRACT

The union of Abell and Abell-Corwin-Olowin samples of rich clusters provides a view of the universe up to $z \sim 0.1$ and within this domain there are two outstanding concentrations of clusters. The nearer of these, the *Shapley concentration* $140 h^{-1}$ Mpc from us, lies close to the direction of our motion inferred from the microwave dipole, suggesting that coherent streaming may extend over this great scale. In addition, there are two startling geometric results: (1) the previously announced concentration of rich clusters to the supergalactic equator extends across a domain of $\sim 450 h^{-1}$ Mpc, representing a $\sim 6 \sigma$ deviation from a Poissonian distribution and a $\sim 3 \sigma$ deviation when clustering is allowed for with a simple model. (2) The Broadhurst et al. “periodicities” in galaxy redshifts anticipate where there are concentrations of clusters and the correspondence orthogonal to the line of sight of their probes appears to be maintained on scales up to $400 h^{-1}$ Mpc. These surfaces are orthogonal to the entity on the supergalactic equator. However, they constitute only a small perturbation to the overall cluster distribution, consistent with fluctuations in the cosmic microwave background of $\Delta T/T \approx 10^{-5}$ on angular scales of $\sim 1^\circ$.

Subject headings: cosmology: observations — galaxies: clustering — large-scale structure of universe

1. INTRODUCTION

There have been controversial suggestions that there are structures on a scale of $0.1c$ lying in the plane of the Local Supercluster (Tully 1986, 1987, hereafter T86 and T87) and of periodicity in galaxy clustering at intervals of $130 h^{-1}$ Mpc² (Broadhurst et al. 1990, hereafter BEKS), and that the *Shapley concentration* at $140 h^{-1}$ Mpc might be a significant source of attraction contributing to the motion inferred from the microwave background dipole (Scaramella et al. 1989, henceforth SBCVZ; Raychaudhury 1989; Scaramella, Vettolani, & Zamorani 1991, hereafter SV2). We will present preliminary new information that provides some support for all of these startling claims. There are hints that very thin structures on the scale of several hundred megaparsecs are common and that intersections between filaments tend to be strikingly near to right angles. There is a remarkable adherence of structures to the cardinal directions of the supergalactic coordinate system introduced by de Vaucouleurs & de Vaucouleurs (1964), which was based on the local galaxy distribution.

These claims go well beyond the now-popular view of a universe made up of a network of interconnecting filaments which might be described within a framework of correlated clustering on scales up to only a few tens of megaparsecs. An organization, or casual connectedness, could be implied on scales of 10%–20% of the current light horizon. We think that

the present evidence, although far from being conclusive, should be presented to fuel further investigation of these problems.

2. NEW DATA

We are mapping large-scale structure using rich clusters which have the tandem advantages that they can be easily identified at large distances and that they highlight regions of extreme density. Recently, Abell, Corwin, & Olowin (1989, hereafter ACO) have published a list of clusters identified on the ESO/SERC survey plates of the southern sky which complements the earlier Abell (1958) survey of the north, resulting in full coverage of the unobscured sky. Scaramella et al. (1991; also Batuski et al. 1989) have studied the properties of these combined catalogs including incompleteness characteristics as functions of richness, distance, latitude, and declination and homogeneity (or lack thereof) between the northern and southern material. The critical point for the present discussion is that for the ACO clusters it is possible to estimate distances from the magnitudes of the third and tenth brightest members to an accuracy of $\pm 20\%$ rms out to $z \sim 0.2$ – 0.25 (see Zamorani et al. 1992). This good news means that we can take an exploratory look at the vast volume of space covered by this survey even though the present redshift information provides only spotty coverage. By contrast, it is confirmed that for the old Abell sample the photometrically estimated distances fail totally beyond $300 h^{-1}$ Mpc.

Scaramella et al. (1991) found that the north and south samples are not homogeneous with the ACO sample probably

¹ Postal address.

² Here $h = H_0/100$ where H_0 is the Hubble constant. Comoving distances are given in an Einstein–de Sitter universe ($\Omega_0 = 1$).

more complete, so it would be unwise to make much out of large-scale north-south asymmetries. Also, where we make use of photometric distance estimates we might create a variation of the “finger of God” artifact—extended apparent features which point at us. The ACO catalog is limited to $\delta < -17.5^\circ$, or approximately a third of the sky. The Abell catalog limit is $\delta > -27^\circ$ but in the overlap zone we use the higher quality ACO catalog. In the following, what we mean by the “Abell catalog region” will be restricted to $\delta > -17.5^\circ$.

3. A DOMINANT PLANE WITHIN $0.1c$

In T86 and T87 there was a discussion of the coincidence of an excess of rich clusters within $30,000 \text{ km s}^{-1}$ to the plane of the Local Supercluster defined by de Vaucouleurs and de Vaucouleurs (1964; de Vaucouleurs 1953, 1956) based on the distribution of galaxies characteristically within 3000 km s^{-1} . Indeed, Zel’dovich, Einasto, & Shandarin (1982) and Einasto et al. (1983) had already noticed that clusters out to the distance of Coma, at 7000 km s^{-1} , lie preferentially in this plane. As things stood at the time of these earlier publications, there was an excess of ~ 35 clusters above random expectations and a “signal” of $\sim 4 \sigma$ significance compared with a random distribution. The Sheckman (1985) sample gave a more pronounced signal but with a modest number of clusters. The main contribution to this signal in both cases came from what was called the Pisces-Cetus supercluster at $18,000 \text{ km s}^{-1}$ near the south Galactic pole.

We know that clusters are *not* randomly distributed and the cluster-cluster correlation length is $14\text{--}25 h^{-1} \text{ Mpc}$ (Bahcall & Soneira 1983; Huchra et al. 1990). It was already admitted in T87 but Postman et al. (1989) demonstrated the point more rigorously that a possible alternative to coherence over several hundreds of megaparsecs was chance alignment of a small number of superclusters each individually with scales of several tens of megaparsecs. With this explanation, the coincidence with the plane of the Local Supercluster is fortuitous, but the probability of that happening with the earlier sample was not so small. Postman, Huchra, & Geller (1992) have restated the Postman et al. assertion with a sample that is slightly enlarged but still confined to the north and the subset of clusters with measured redshifts.

The new sample of ACO clusters with $\delta < -17.5^\circ$ plus additional Abell clusters with photometric distances within $300 h^{-1} \text{ Mpc}$ can be used to test the earlier hypothesis that there is something special about the supergalactic equator on scales far larger than the domain of nearby galaxies. If it were correct that the concentration of clusters to this plane is a coincidence of the placement of a few intermediate-scale superclusters then augmentation of the sample to include the southern sky and greater distances should wash out the apparent effect. Instead, *the signal is spectacularly strengthened.*

We will discuss an all-sky Abell/ACO sample of 715 clusters restricted to $300 h^{-1} \text{ Mpc}$. Either using the entire volume or a somewhat restricted part of the volume there is an excess of ~ 45 clusters over random expectations confined narrowly to the supergalactic equator. Figure 1 shows this signal in a sphere of radius $220 h^{-1} \text{ Mpc}$, where the origin ($\text{SGX} = -40$, $\text{SGY} = -80$, $\text{SGZ} = 0 h^{-1} \text{ Mpc}$) has been displaced from our position in order to optimize the ratio of the number of clusters on the plane to the total. The cluster excess is sharply confined in three bins centered around $\text{SGZ} = -10 h^{-1} \text{ Mpc}$. This excess is 6σ above $N^{1/2}$ expectations for a random distribution.

We can check whether this increased signal is still compatible with the Postman et al. (1989) hypothesis based on the established notion of a clustering of clusters of galaxies. Here, we give a simple analytical estimate, leaving the check against detailed simulations to a future study. For a set of objects which have a clustered distribution obeying a spatial two-point correlation function ξ , the expected variance in number counts is enhanced by a constant factor with respect to the uncorrelated Poisson case: $\langle (N_c - \langle N_c \rangle)^2 \rangle = \langle N_c \rangle (1 + q)$, where $q = 4\pi n_c J_3$, n_c is the number density, and $J_3 \equiv \int dr r^2 \xi(r)$. Assuming now that clusters of richness class $R \geq 0$, have correlation length $r_0 = 20 h^{-1} \text{ Mpc}$, with a slope of $\gamma = -1.8$ for ξ , and that there is negligible correlation on large scales, i.e., $\xi(r \geq 50 h^{-1} \text{ Mpc}) \approx 0$, we find that $q \sim 3.5$. Therefore the “number of sigmas” is now reduced to 2.8. This is much less striking than the Poissonian value, but it is still on the high side and cannot be lightly dismissed. The T86, T87 discussion has the consequence that the signal should be evaluated as an a priori expectation.

The minor displacement of the origin for the data in Figure 1

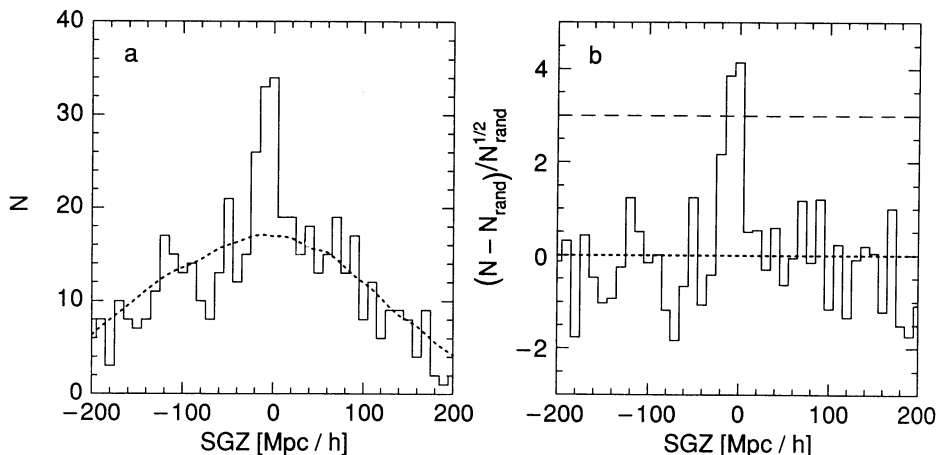


FIG. 1.—(a) Number of clusters in $10 h^{-1} \text{ Mpc}$ SGZ bins in a sphere of radius $220 h^{-1} \text{ Mpc}$ about $\text{SGX}_0 = -40$, $\text{SGY}_0 = -80$, $\text{SGZ}_0 = 0 h^{-1} \text{ Mpc}$. The curved baseline is given by the average of 100 random catalogs with the selection function of the real data. The curvature is due to geometry, the effects of galactic obscuration, and a small notch in the sphere at distances $> 300 h^{-1} \text{ Mpc}$. (b) The baseline curvature has been removed. The ordinate is $(N_{\text{signal}} - N_{\text{random}}) / (N_{\text{random}})^{1/2}$ for a single bin.

is a reflection of our finding that, while contribution to the apparent concentration to the supergalactic plane arises over a vast region, it does *not* come from everywhere within $300 h^{-1}$ Mpc. The main contributions come from two regions: the Pisces-Cetus region previously recognized although now followed farther south and the Shapley concentration, first discussed in modern time by SBCVZ and Raychaudhury (1989) but found by the latter to have come to the attention of Shapley (1930). Other exceptional aspects of this region have been noted by Lahav et al. (1989) and Allen et al. (1990).

These two distinct regions are well separated on opposite sides of the zone of obscuration. The Pisces-Cetus supercluster is centered in the zone of overlap between the Abell and ACO surveys ($-17.5 < \delta < -27^\circ$) and a common picture emerges from the two catalogs. The structure breaks into several lumps extending across $\sim 250 h^{-1}$ Mpc within the narrow plane. By contrast, the Shapley concentration is dominated by a single region of very high cluster density, with 29 ACO clusters within a sphere of radius $50 h^{-1}$ Mpc. There is only one other similarly large concentration of rich clusters within $30,000 \text{ km s}^{-1}$ of our position: the region called the Horologium-

Reticulum supercluster of the following maps. Fairall & Jones (1988) call this region the Further Horologium supercluster. This part of the sky has been studied by Lucey et al. (1983) and was already noted as exceptional by Shapley (1935).

A projection of the distribution of clusters within a box of $400 h^{-1}$ Mpc on a side is seen in Figure 2. The projection onto the SGX-SGZ plane illustrates the distinct Pisces-Cetus and Shapley components that adhere to the supergalactic equator. The Horologium-Reticulum supercluster is seen below this plane. The most remarkable additional feature of the map is a second ridge of clusters at more negative SGX values from the Pisces-Cetus region which extends over $\sim 200 h^{-1}$ Mpc parallel to the equatorial plane but offset of $\text{SGZ} \sim 30 h^{-1}$ Mpc. The clusters in this feature do *not* contribute to the signal identified in Figure 1 coincident with the equator and the feature is not substantial enough to generate a significant additional signal.

4. GIANT ORTHOGONAL STRUCTURES?

We were curious to look at what is going on in the cluster distribution at the periodic peaks reported by BEKS as

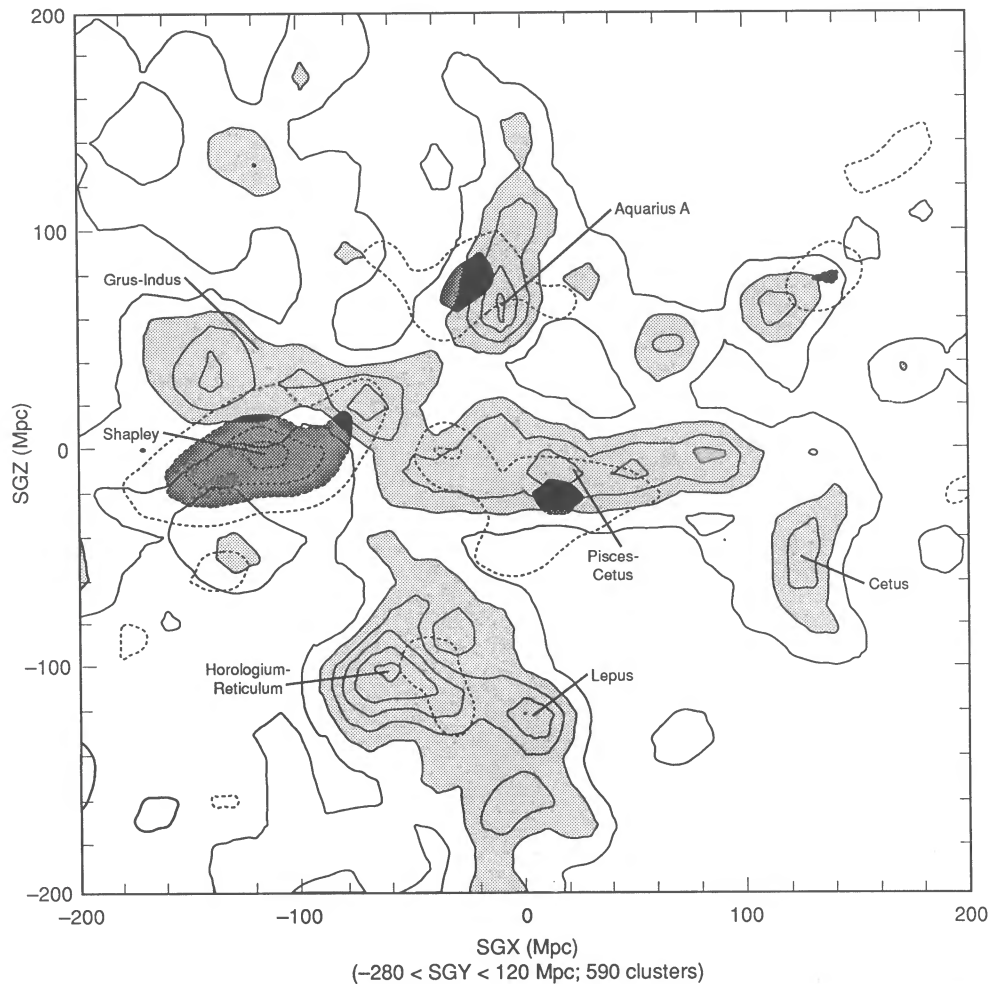


FIG. 2.—An SGX-SGZ view of structure in a $400 h^{-1}$ Mpc box with 590 clusters that contains the region contributing to the signal in Fig. 1. The projection is actually the sum of a south Galactic cube ($-280 < \text{SGY} < 0 h^{-1}$ Mpc: solid contours and light gray shades) and a north Galactic cube ($0 < \text{SGY} < 120 h^{-1}$ Mpc: dashed contours and dark gray shades). Contours are from Gaussian smoothing with $10 h^{-1}$ Mpc scale-length and are in units of 10^{-3} clusters Mpc^{-2} with the first shaded levels at 2×10^{-3} . The signal in Fig. 1 at $\text{SGZ} \sim 0$ is basically the sum of contributions from the Pisces-Cetus supercluster south of the Galactic plane ($\text{SGY} < 0$) and the Shapley concentration north of the Galactic plane ($\text{SGY} > 0$).

Bahcall (1991) has independently done with a more restricted sample. The direction of the BEKS skewers toward the Galactic poles are within the Abell region in the north and within the ACO region in the south. The deep redshift skewers are *almost in the supergalactic equatorial plane*. To be precise, by construction the SGX axis lies along the intersection of the Galactic and supergalactic planes, these two planes forming an angle of $83^\circ.7$, so the BEKS polar skewers deviate by only $6^\circ.3$ from the SGY axis in supergalactic coordinates.

A few selected maps are shown in Figures 3–5 where we include ACO clusters out to great distances because of the relative reliability of the photometric distance estimate for the southern sample. The high-density regions identified on these maps are listed in Table 1. Figure 3 is an SGY-SGZ projection of a relatively thin ($130 h^{-1}$ Mpc) slice in SGX which includes the BEKS skewer. The BEKS periodicities and the Great Wall (Geller & Huchra 1989) are located. This latter feature stands out in the distribution of individual galaxies but spans a relative gap in the cluster distribution, bridging cluster concentrations. Only part of the objects contributing to the signal at $SGZ \sim 0$ are seen here (for example, the Shapley concentration is not in this SGX window) but an equatorial belt can still be discerned.

Figure 4 illustrates the $50 h^{-1}$ Mpc slab that contains the $SGZ \sim 0$ signal. The BEKS skewer is within this slab and the periods are identified. The location of the “Great Wall” near

the first positive (north) BEKS period is indicated. Interestingly, in the closest BEKS period in the south there is a comparable Cetus Wall (Fairall et al. 1990; Pellegrini et al. 1990 who call this feature “the wall”). This structure lies within the supergalactic equatorial concentration. There are hints of a tendency for objects to align with the cardinal axes of the supergalactic coordinate system as first revealed by the distribution of relatively nearby galaxies. See Tully’s (1988) Figure 1 of the Local Supercluster and the related discussion of the “louvered wall” on an SGX-SGZ surface.

In Figure 5 there is a projection of the whole merged catalog at south Galactic latitudes onto the SGX-SGZ plane. The boundary between the Abell and ACO samples is evident. The BEKS skewer is essentially perpendicular to the page in this view. This fanciful figure hints at structure on the largest scales accessible to the sample.

Our maps are coarse but they are consistent with the picture of interconnected filaments (Einasto, Jõeveer, & Saar 1980) and walls (Geller & Huchra 1989). The daring question asked by BEKS is whether there is some coherence in this network on extraordinarily large scales, and we now ask if this extends in transverse directions with respect to the BEKS skewer axis.

Figure 6a is in the spirit of Figure 1. It is a plot of cluster counts projected onto the SGY axis, drawing from a cylinder of radius $200 h^{-1}$ Mpc concentric with the SGY axis. Clusters contributing to the shaded histogram have measured redshifts

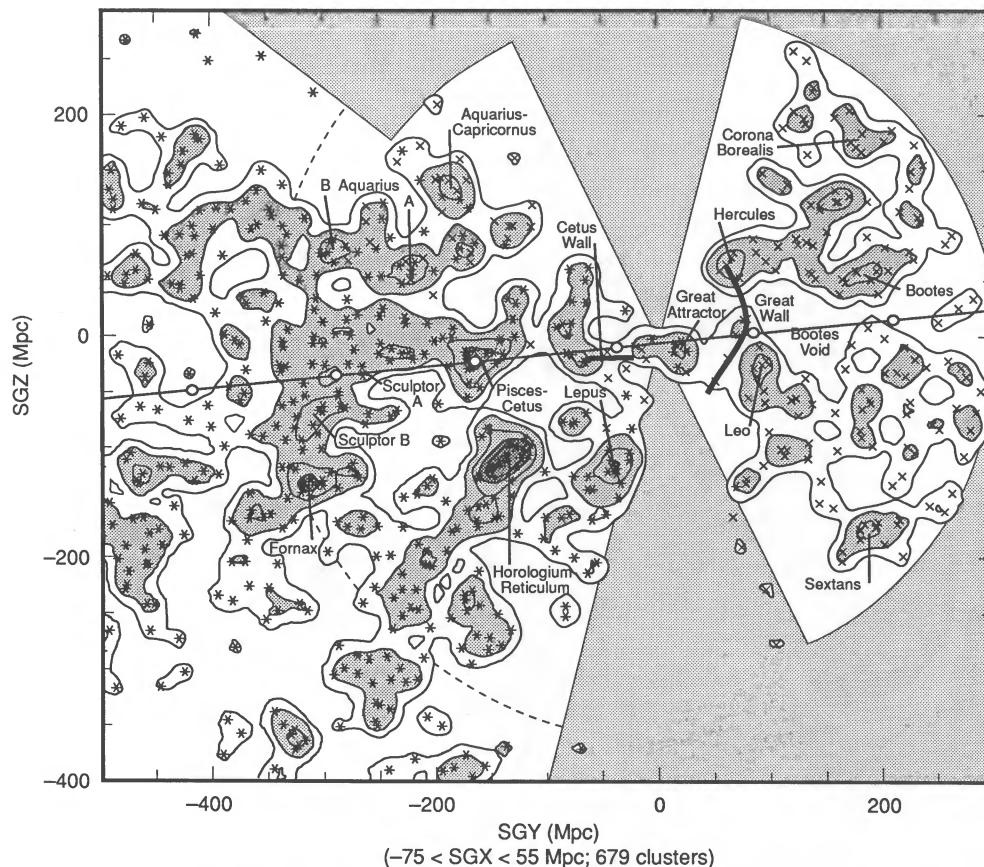


FIG. 3.—An SGY-SGZ projection of a slab $130 h^{-1}$ Mpc thick in SGX. The BEKS probe line is shown (6° from horizontal passing through the origin). Six knots on this line locate BEKS cycle peaks. Individual ACO (*) and Abell (x) clusters are plotted, as well as surface density contours in units of 10^{-3} clusters Mpc^{-2} (first shaded contour at 2×10^{-3} ; darker shade at 4×10^{-3}). Zones of incompleteness due to obscuration and the Abell region limit are indicated. The Great Wall and Cetus Wall are superposed schematically. The dashed curve at a radius of $350 h^{-1}$ Mpc delineates the region of reasonable completion with the ACO sample.

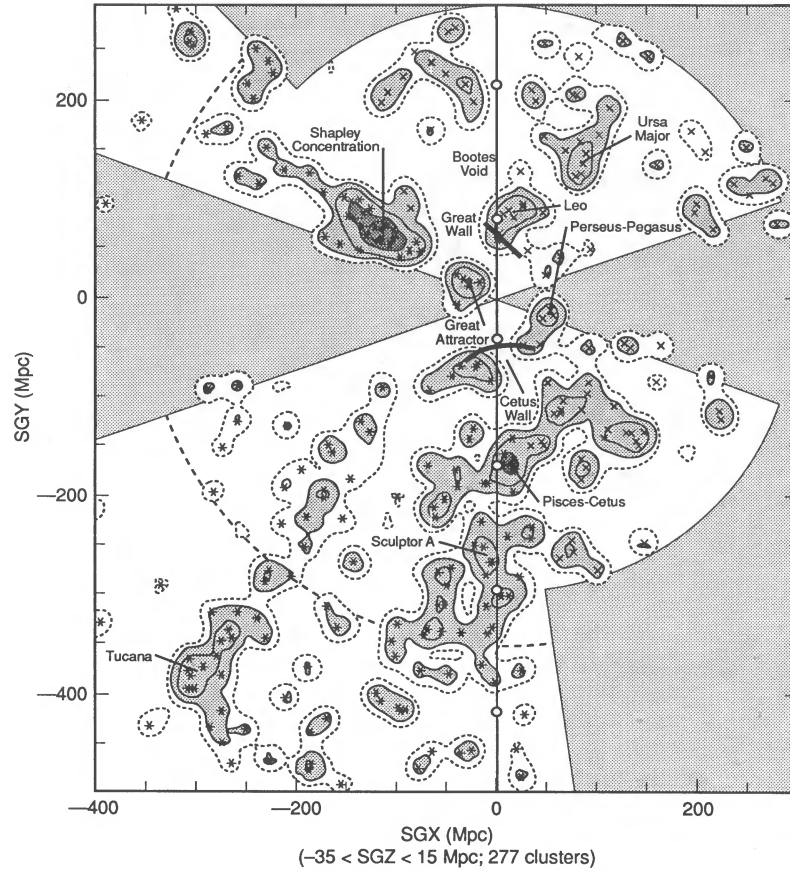


FIG. 4.—An SGX-SGY projection of a slab $50 h^{-1}$ Mpc thick which includes the structures that make up the SGZ ~ 0 signal. One can see the BEKS probe line (passing vertically through origin) and six cycle peaks (knots in line). The Great and Cetus walls are indicated. The first and second contour shade steps are at 1 and 3×10^{-3} clusters Mpc^{-2} . The dashed contour is at a level of 0.5×10^{-3} .

TABLE 1
SUPERCLUSTERS INDICATED IN THE FIGURES

Name	z	α	δ	SGX (Mpc)	SGY (Mpc)	SGZ (Mpc)	Clusters within 25 Mpc	Clusters within 50 Mpc
Great Attractor ^a	0.014	13 ^h 45 ^m	-30°	-36	19	-2	5	6
Perseus-Pegasus ^b	0.018	2 23	42	50	-15	-3	3	7
Leo ^b	0.032	11 25	27	12	90	5	5	14
Hercules ^b	0.037	16 03	17	-25	70	80	6	12
Lepus	0.041	5 45	-26	-10	-40	-110	5	14
Shapley	0.047	13 25	-31	-117	68	-4	12	29
Pisces-Cetus ^b	0.059	0 37	-23	10	-170	-8	6	14
Ursa Major ^b	0.059	11 45	55	85	145	10	7	10
Horologium-Reticulum ^c	0.063	3 14	-48	-55	-135	-105	16	25
Bootes ^b	0.067	13 47	28	-5	180	65	6	12
Corona Borealis ^b	0.072	15 21	28	-5	160	130	7	12
Grus-Indus	0.077	21 20	-55	-140	-160	30	7	15
Aquarius-Capricornus ^b	0.083	22 08	-12	-5	-190	135	5	12
Aquarius A ^b	0.086	23 11	-22	-12	-230	70	7	17
Sextans ^b	0.089	9 47	4	-20	185	-170	2	12
Sculptor A	0.093	0 35	-29	-15	-260	-25	4	14
Cetus	0.094	1 51	-1	125	-220	-65	6	12
Aquarius B	0.109	23 14	-22	-12	-290	80	7	18
Sculptor B	0.117	1 15	-37	-45	-310	-70	4	15
Fornax	0.126	1 58	-31	13	-320	-130	8	16
Tucana	0.175	23 03	-60	-280	-370	-6	4	15
Great Wall	0.021 to 0.033	9 00 to 16 00	+20 to +20	16 to -16	43 to 62	-42 to 73
Cetus Wall ^d	0.017 to 0.025	2 00 to 1 00	+10 to -50	32 to -27	-36 to -66	-11 to -17

^a Also called Hydra-Centaurus or Virgo-Hydra-Centaurus supercluster.

^b In T87.

^c Also called Further Horologium supercluster.

^d Also called "The Wall."

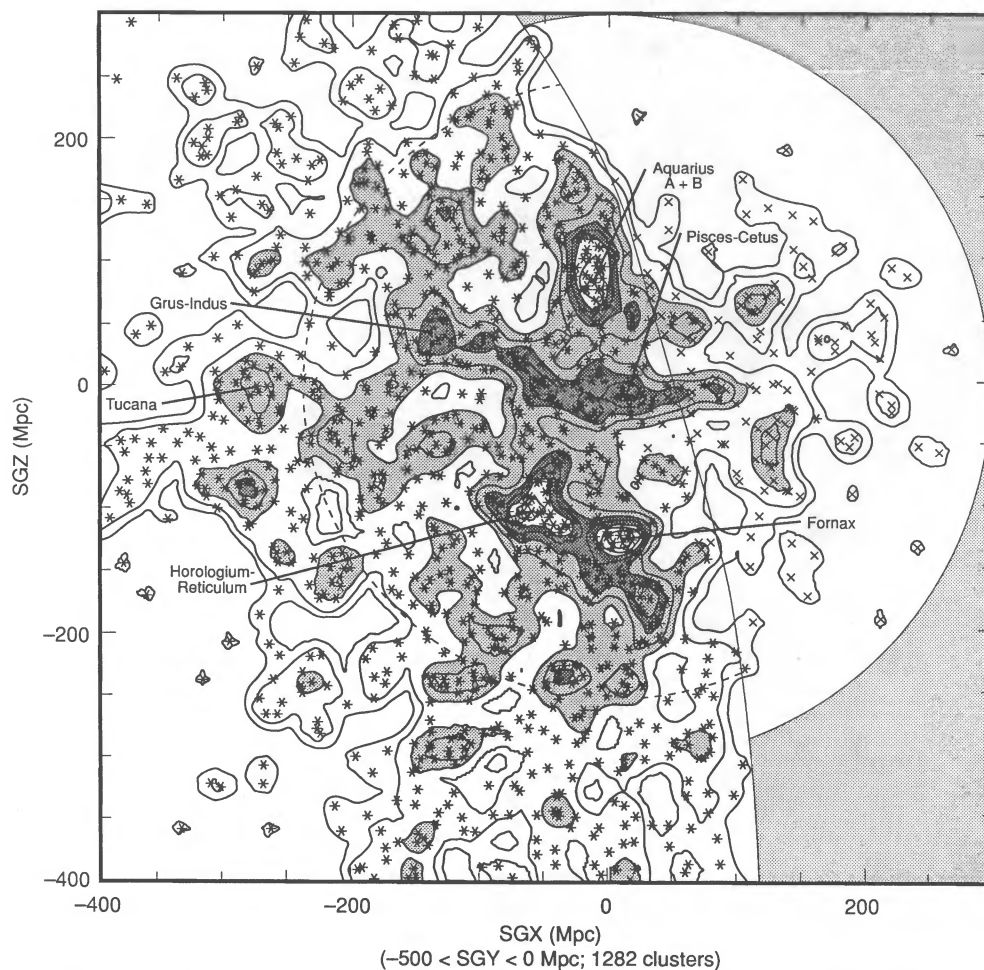


FIG. 5.—An SGX-SGZ projection of the entire southern Galactic sky ($SGY < 0$). The ACO declination limit of $-17^{\circ}5$ and Abell distance limit of $300 h^{-1}$ Mpc are indicated (The Abell domain is actually limited by Galactic obscuration in this projection). First shaded contour is now 3×10^{-3} , darker contour at 5×10^{-3} , and return to white at 7×10^{-3} clusters Mpc^{-2} .

while the rest have only photometric distance estimates. The dotted line shows the mean of simulated data obeying our selection function. The bins are phased with the BEKS periodicities with 6 bins/cycle.³

Figure 6b displays the number excess of the same data with respect to the smoothed baseline provided by the simulations. The vertical dashed lines locate the periodicity maxima delineated by BEKS. It is evident that BEKS are able to predict reasonably well where there are excesses in the cluster counts in the orthogonal directions.

Figure 6c shows the same information as Figure 6b but stacks the separate cycles on top of each other. The phases and cycle length are strictly as prescribed by BEKS. The dotted line in Figure 6c is based only on clusters within $100 h^{-1}$ Mpc of the SGY axis, while the solid line is based on clusters within $200 h^{-1}$ of the SGY axis. The difference reveals that the signal continues to grow on scales between a cylinder radius of $100 h^{-1}$ Mpc and a radius of $200 h^{-1}$ Mpc. With respect to Poisson statistics, the maximum and minimum bins achieve

$\pm 3 \sigma$ significance (one bin at maximum; two bins at minimum).

A power spectrum of data in Figure 6b is shown in Figure 6d. The peak at five cycles implies there is power on the dimensions of our cylinder of $600 h^{-1}$ Mpc divided by five cycles, hence $\sim 120 h^{-1}$ Mpc. The points with error bars denote the expected values in a pure Poissonian case, while the dotted-dashed line denotes the maximum values found out of 100 pure Poissonian cases.

A power spectrum of data in Figure 6b is shown in Figure 6d. The peak at five cycles implies there is power on the dimensions of our cylinder of $600 h^{-1}$ Mpc divided by five cycles, hence $\sim 120 h^{-1}$ Mpc. The points with error bars denote the expected values in a pure Poissonian case, while the dotted-dashed line denotes the maximum values found out of 100 pure Poissonian cases.

Of course, it would have been unjustified to turn the process around and predict periodicity with the present restricted data set. The BEKS statistics are better. There are additional peaks, and the coincidences are broad. However, one can be attracted by the possibility that the coincidences are real. If so, though, then there must be huge structures because the peaks in Figure 6b and the power spectrum in Figure 6d grow as the radius of the sampling cylinder about the SGY axis is increased up to $200 h^{-1}$ Mpc.

³ We are testing a thesis that there is something special about the supergalactic coordinate system, so we project the BEKS skewer the small amount to the SGY axis. After all, their direction was chosen only because it is toward the pole of our Galaxy.

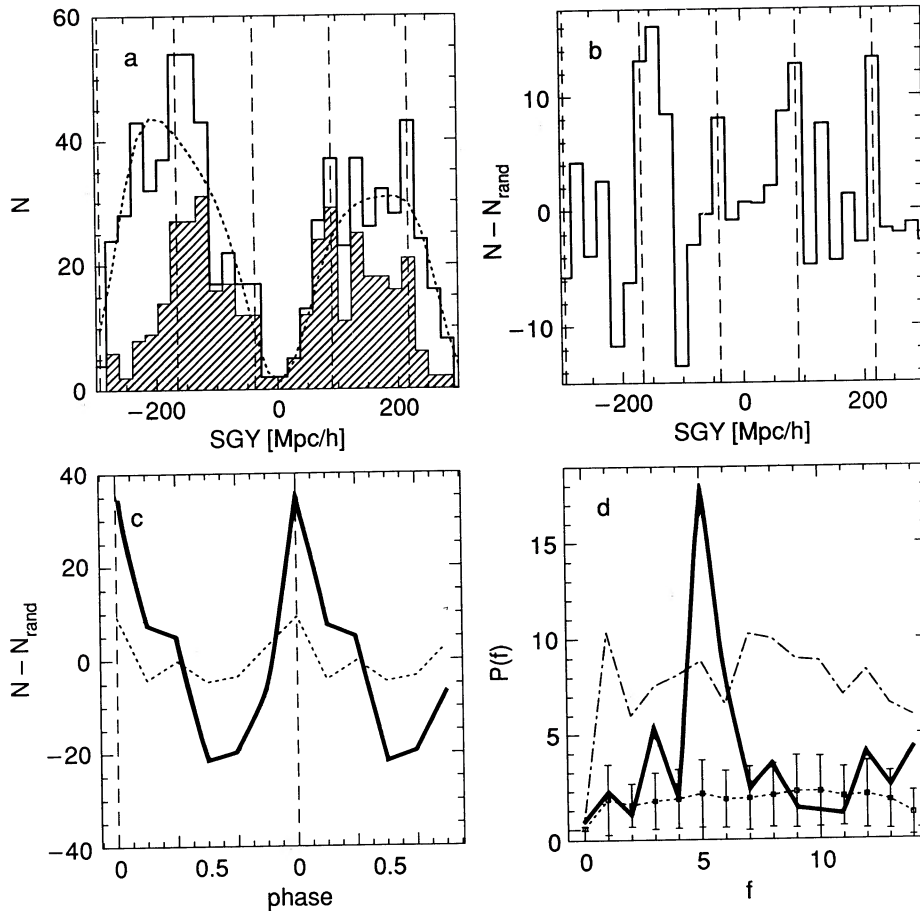


FIG. 6.—(a) Number of clusters in $128/6 h^{-1}$ Mpc SGY bins within a cylinder of radius $200 h^{-1}$ Mpc centered on the SGY axis. Shaded histogram: fraction of clusters with distances established by redshifts. Dotted curve: expected distribution based on average of 100 simulated data sets obeying selection function of the real data set. Dashed vertical lines are at projected SGY positions of BEKS periodicity peaks. (b): Normalized histogram based on the expectation distribution. The ordinate indicates the number excess per bin. (c) Histogram comparable to (b) but with the separate cycles superposed and repeated once for better clarity. BEKS peaks are at phase zero. The dotted line denotes clusters within a radius of $100 h^{-1}$ Mpc of the SGY axis, while the solid line those within a radius of $200 h^{-1}$ Mpc of the SGY axis. (d) Power spectrum of (b). Points with errors bars come from 100 simulated data sets, while the dotted-dashed line shows the maximum values attained in these sets.

One can look again at where the BEKS periods peak in the skewers located in Figure 3 and 4. Though the maps are usually busy at the BEKS peak signal locations, these spots do not look particularly special. It is seen that with only cluster tracers the hypothesized structures are the sums of subunits without obvious connections.

5. SUMMARY

1. With the extended sample, the signal on the supergalactic equator has grown from 4σ to 6σ significance compared with a random distribution. Contributions come in roughly equal parts from the extended Pisces-Cetus region south of the Galactic plane and the dense Shapley concentration north of the Galactic plane. The signal on the supergalactic equator has $\Delta\text{SGZ}_{\text{FWHM}} = 18 h^{-1}$ Mpc, centered at $\text{SGZ}_0 = -5 h^{-1}$ Mpc, and draws on clusters over a domain of $\sim 450 h^{-1}$ Mpc $\sim 0.17c$. There was no information about the Shapley concentration at the time of the discussion in T86 and T87, so the fact that this feature lies elongated precisely in the same plane that was discussed earlier stretches the tenability of the coincidence hypothesis even in the presence of a correlated distribution. In fact, the significance of such excess is still quite noteworthy

($\sim 3\sigma$) when we make allowance for clustering up to $50 h^{-1}$ Mpc with a simple model.

2. Within the unobscured portion of the volume within $300 h^{-1}$ Mpc, there are two outstanding regions in the celestial south where the number of clusters within spheres of diameters up to $150 h^{-1}$ Mpc are higher than anywhere else (see Table 1). The closer of these, the Shapley concentration, is roughly in the direction of the cosmic microwave background (CMB) dipole anisotropy. Scaramella et al. (1991), SVZ, and Plionis & Valdarnini (1991) have demonstrated that the dipole in the distribution of Abell/ACO clusters points in this same direction and the acceleration vector reaches a plateau on the distance scale of this aggregate. It would be surprising if this agreement between the two dipole directions is a coincidence (SVZ estimate such probability to be $\sim 2 \times 10^{-3}$). If it is not a coincidence, there is a significant attraction at our position from a concentration of objects at a distance of $140 h^{-1}$ Mpc, as initially suggested by SBCVZ. Shaya, Tully, & Pierce (1992) also invoke a contribution from this region in their model of large-scale flows, a prospect supported by the observations of bulk flow by Mathewson, Ford, & Buchhorn (1992). Willick (1990) argues the coherence extends in the opposite direction

by 5500 km s^{-1} to the Perseus supercluster. Because of the extreme adhesion to a single plane, *causality* could extend to the Pisces-Cetus supercluster, across $50,000 \text{ km s}^{-1}$.

3. The BEKS periodicity peaks in narrow skewers anticipate where maxima are observed in the distribution of rich clusters (four good cycles), a situation also pointed out by Bahcall (1991). It is noteworthy that these innermost cycles were poorly sampled by BEKS and did not play a dominant role in the establishment of their postulate of periodicity. The phase-combined maxima and minima have $\pm 3 \sigma$ Poisson significance. This is not a substantial signal if it were identified a posteriori since the significance would be reduced if compared with a model with built-in correlations. However, it is impressive given that the cycle and phase are prescribed by BEKS. If the correspondence is taken seriously, then there is inferred evidence for structures on scales *perpendicular* to the BEKS probes of up to $\sim 400 h^{-1} \text{ Mpc}$ diameter *since the signals corresponding to the periodicity continue to grow up to this scale*. These structures are *orthogonal* to the plane at $\text{SGZ} \sim 0$.

4. An immediate problem if these structures are real is raised by the observed smoothness of the CMB, since perturbations should arise if there are substantial mass fluctuations on these large scales. However, it is to be noted that this signal does *not* constitute a strong perturbation to the overall distribution of the sample we have examined. In SVZ we show that the Abell/ACO sample asymptotically yields to an isotropic distribution, while still being consistent with a cellular structure of appropriate scales (Zamorani et al. 1992). From Figure 6b we see that the signal, folded over four cycles, can be very roughly represented as a sinusoid of wavelength $\lambda_0 \sim 130 h^{-1} \text{ Mpc}$ and of amplitude ~ 35 clusters, compared with a total of 715 clusters within the same volume. It follows that this is a small ripple, $\delta N_c/N_c \sim 5 \times 10^{-2}$, perhaps indicating the presence of a spike in the power spectrum at λ_0 . The corresponding mass

fluctuation is $\delta_0 \equiv \delta M/M \sim b_{cp}^{-1} \delta N_c/N_c \sim 1-1.5 \times 10^{-2}$, where $b_{cp} \sim 3-5$ is the biasing factor of clusters with respect to the matter. We can give some order of magnitude estimates of the expected level of temperature fluctuations normalized to the case $\Omega_0 = 1$, assuming standard recombination with the redshift of last scattering surface $z_{LS} \sim 10^3$, and horizon scale $r_0 = 2c/H_0$. The effects of interest here are potential fluctuations (Sachs-Wolfe effect) and velocity induced fluctuations at the last scattering surface, which would give rise to temperature anisotropies on an angular scale of $\sim 1^\circ \Omega_0$. The former yields $\Delta T/T \sim (1/3)(\lambda_0/r_0)^2 \delta_0 \Omega_0 f(\Omega_0) \approx 2 \times 10^{-6} \Omega_0^{0.3}$, while the latter gives $\Delta T/T \sim (\lambda_0/r_0) \delta_0 [1 + z_{LS}]^{-1/2} \Omega_0^{1/2} f(\Omega_0) \approx 10^{-5} \Omega_0^{-0.2}$ [the function $f(\Omega_0) \approx \Omega_0^{-0.7}$ reflects the less efficient growth of linear perturbations in an open universe]. These are rough approximations but indicate values that are in an interesting range, potentially within reach of present experiments on angular scales of one degree (e.g., Vittorio et al. 1991).

The present unsatisfactory observational situation will only be rectified by very deep and very wide field redshift surveys. We have made predictions here that must be tested with more rigorously defined samples. If the hints we have are correct, there is an organization to large scale structure on scales of 10%–20% of the light horizon and it is of a nature that current gravity models do not predict. In a blush of conservatism, the title of this article was altered from the first choice: “A three-dimensional Chessboard Universe?” In our imagination, the Great Wall figurine is only a pawn and the warrior in Figure 5 is a more important piece.

We thank N. Vittorio for useful discussions. This research was partially supported by a grant from the US National Science Foundation.

REFERENCES

- Abell, G. O. 1958, *ApJS*, 3, 211
 Abell, G. O., Corwin, H. G., Jr., & Olowin, R. 1989, *ApJS*, 70, 1 (ACO)
 Allen, D. A., Norris, R. P., Staveley-Smith, L., Meadows, V. S., & Roche, P. F. 1990, *Nature*, 343, 45
 Bahcall, N. A. 1991, *ApJ*, 376, 43
 Bahcall, N. A., & Soneira, R. M. 1983, *ApJ*, 270, 20
 Batuski, D. J., Bahcall, N. A., Olowin, R. P., & Burns, J. O. 1989, *ApJ*, 341, 599
 Broadhurst, T. J., Ellis, R. S., Koo, D. C., & Szalay, A. S. 1990, *Nature*, 343, 726 (BEKS)
 de Vaucouleurs, G. 1953, *AJ*, 58, 30
 ———. 1956, *Vistas Astron.*, 2, 1584
 de Vaucouleurs, G., & de Vaucouleurs, A. 1964, *Reference Catalogue of Bright Galaxies* (Austin: University of Texas Press)
 Einasto, J., Jõeveer, M., & Saar, E. 1980, *MNRAS*, 193, 353
 Einasto, J., Corwin, H. J., Jr., Huchra, J. P., Miller, R. H., & Tarenghi, M. 1983, *Highlights Astron.*, 6, 757
 Fairall, A. P., & Jones, A. 1988, *Publ. Dept. Astron. Univ. Cape Town*, No. 10
 Fairall, A. P., Palumbo, G. G. C., Vettolani, G., Kauffmann, G., Jones, A., & Baiesi-Pillastrini, G. 1990, *MNRAS*, 247, 21P
 Geller, M. J., & Huchra, J. P. 1989, *Science*, 246, 897
 Huchra, J. P., Henry, J. P., Postman, M., & Geller, M. J. 1990, *ApJ*, 365, 66
 Lahav, O., Edge, A. C., Fabian, A. C., & Putney, A. 1989, *MNRAS*, 238, 881
 Lucey, J. R., Dickens, R. J., Mitchell, R. J., & Dawe, J. A. 1983, *MNRAS*, 203, 545
 Mathewson, D. S., Ford, V. L., & Buchhorn, M. 1992, *ApJL*, submitted
 Pellegrini, P. S., da Costa, L. N., Huchra, J. P., Latham, D. W., & Willmer, C. N. A. 1990, *AJ*, 99, 751
 Plionis, M., & Valdarnini, R. 1991, *MNRAS*, 249, 46
 Postman, M., Huchra, J. P., & Geller, M. J. 1992, *ApJ*, 384, 404
 Postman, M., Spergel, D. N., Sutin, B., & Juskiewicz, R. 1989, *ApJ*, 346, 588
 Raychaudhury, S. 1989, *Nature*, 342, 251
 Scaramella, R., Baiesi-Pillastrini, G., Chincarini, G., Vettolani, G., & Zamorani, G. 1989, *Nature* 338, 562 (SBCVZ)
 Scaramella, R., Vettolani, G., & Zamorani, G. 1991, *ApJL*, 376, L1 (SVZ)
 Scaramella, R., Zamorani, G., Vettolani, G., & Chincarini, G. 1991, *AJ*, 101, 342
 Shapley, H. 1930, *Harvard Obs. Bull.*, 874, 9
 ———. 1935, *Ann. Harvard College Obs.*, 88, 107
 Shaya, E. J., Tully, R. B., & Pierce, M. J. 1992, *ApJ*, submitted.
 Shectman, S. A. 1985, *ApJS*, 57, 77
 Tully, R. B. 1986, *ApJ*, 303, 25 (T86)
 ———. 1987, *ApJ*, 323, 1 (T87)
 ———. 1988, *Vatican Study Week: Large-Scale Motions in the Universe*, ed. V. C. Rubin & G. V. Coyne (Princeton Univ. Press), 71
 Vittorio, N., Meinhold, P., Muciaccia, P. F., Lubin, P., & Silk, J., 1991, *ApJL*, 372, L1
 Willick, J. 1990, *ApJL*, 351, L5
 Zamorani, G., Scaramella, R., Vettolani, G., & Chincarini, G. 1992, in *Traces of Primordial Structure in the Universe*, ed. H. Boeringer & R. A. Tremann, in press
 Zel'dovich, Ya. B., Einasto, J., & Shandarin, S. F. 1982, *Nature*, 300, 407